

Elastic $\bar{p}d$ scattering and total $\bar{p}d$ cross sections reexamined

Yu.N. Uzikov^{1,2} and J. Haidenbauer³

¹*Laboratory of Nuclear Problems,
JINR, 141980 Dubna, Russia*

²*Physics Department, Moscow State University,
119991 Moscow, Russia*

³*Institute for Advanced Simulation and Institut für Kernphysik,
Forschungszentrum Jülich, D-52425 Jülich, Germany*

(Dated: September 7, 2018)

We update our recent analysis of $\bar{p}d$ scattering, performed within the Glauber theory including the single- and double $\bar{p}N$ scattering mechanisms. Specifically, now we consider also $\bar{N}N$ amplitudes from a new partial-wave analysis of $\bar{p}p$ scattering data. Predictions for differential cross sections and the spin observables A_y^d , $A_y^{\bar{p}}$, A_{xx} , A_{yy} are presented for antiproton beam energies between 50 and 300 MeV. Total polarized cross sections are calculated utilizing the optical theorem. The efficiency of the polarization buildup for antiprotons in a storage ring is investigated.

PACS numbers: 25.10.+s, 25.40.Qa, 25.45.-z

Keywords: antiproton-deuteron collisions, spin-dependent antiproton-nucleon interaction

I. INTRODUCTION

Scattering of antiprotons off polarized nuclei can be used to produce a beam of polarized antiprotons by exploiting the so-called spin-filtering effect [1]. The PAX Collaboration intends to utilize scattering of antiprotons off a polarized ^1H target in rings [2] as the basic source for antiproton polarization buildup at an upgrade of the FAIR facility in Darmstadt. In view of the limited information on the spin dependence of the $\bar{p}N$ force, the interaction of antiprotons with a polarized deuteron is also of interest for the issue of the antiproton polarization buildup.

In a recent paper [3] we considered $\bar{p}d$ scattering within the Glauber theory of multi-step scattering [4], taking into account the full spin-dependence of the elementary $\bar{p}N$ scattering amplitudes. Predictions for various observables were given for antiproton beam energies from 50 to 300 MeV employing $\bar{p}N$ amplitudes generated from $\bar{N}N$ potentials developed by the Jülich Group [5–7]. Specifically, the $\bar{p}N$ amplitudes were taken from the models A(BOX) introduced in Ref. [5] and D described in Ref. [7]. Both models provide a very good overall reproduction of the low- and intermediate energy $\bar{N}N$ data as documented in those works. On the other hand, there are clearly visible deficiencies in the description of spin-dependent observables like the analyzing powers, for elastic $\bar{p}p$ scattering but in particular for the $\bar{p}p \rightarrow \bar{n}n$ reaction[7].

While we were preparing our work [3] an updated version of the Nijmegen partial-wave analysis was presented by Zhou and Timmermans [8]. For this new analysis concrete values of the resulting phase shifts and inelasticities are provided in the publication so that we can reconstruct the corresponding $\bar{N}N$ amplitudes and we can employ them for a calculation of $\bar{p}d$ scattering within the Glauber theory. As demonstrated in [8] the $\bar{N}N$ am-

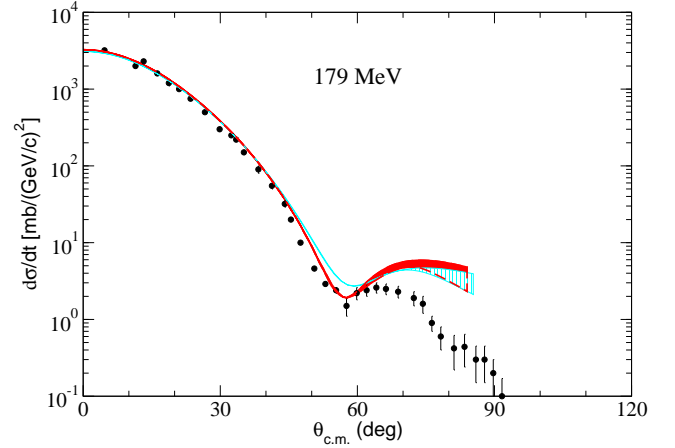


FIG. 1: (Color online) Differential cross section of elastic $\bar{p}d$ scattering at 179 MeV versus the c.m. scattering angle. Results are shown for the $\bar{N}N$ amplitudes of Ref. [8] (cyan/hatched) and of the Jülich model D (red/black). The bands represent the sensitivity to variations of the large-angle tail of the $\bar{p}N$ amplitudes as discussed in the text. The data points are taken from Ref. [12].

plitudes based on those phase-shift parameters yield an excellent description of the experimental data included in the database of the analysis. Thus, they constitute definitely the best and most reliable representation of the $\bar{N}N$ interaction, and specifically of its spin dependence, that we have at hand at the moment. Therefore, it is instructive to investigate the implications of those amplitudes on the various $\bar{p}d$ scattering observables that we considered in our recent paper [3]. Of particular interest are, of course, spin observables such as A_y^d , $A_y^{\bar{p}}$, A_{xx} , A_{yy} . Equally interesting are predictions for the efficiency of the polarization buildup for antiprotons in a storage ring for scattering off a deuteron target. Those are the parameters relevant for the planned experiments

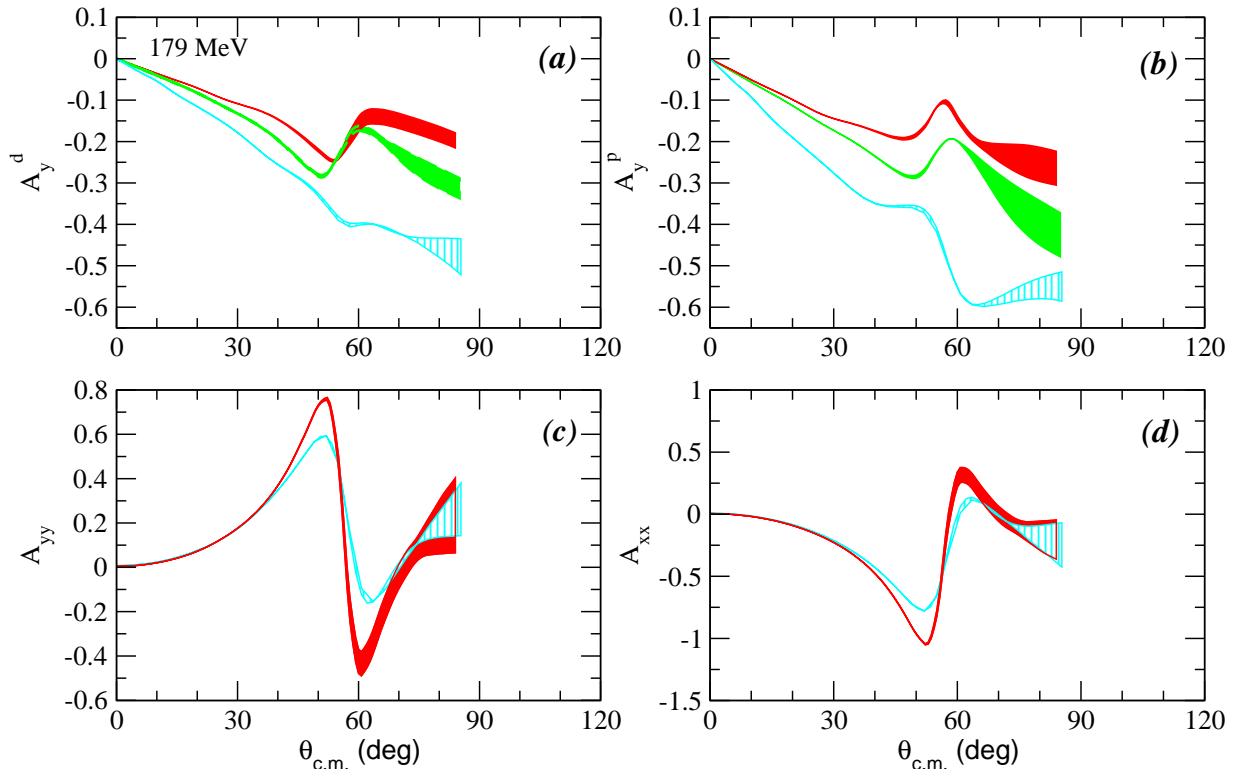


FIG. 2: (Color online) Spin observables of elastic $\bar{p}d$ scattering at 179 MeV versus the c.m. scattering angle: A_y^d (a), A_y^p (b), A_{yy} (c), and A_{xx} (d). Results are shown for the $\bar{N}N$ amplitudes of Ref. [8] (cyan/hatched), and of the $\bar{N}N$ models A (green/grey) and D (red/black). The bands represent the sensitivity to variations of the large-angle tail of the $\bar{p}N$ amplitudes as discussed in the text.

of the PAX Collaboration and it is rather helpful for the preparations of a future experiment to have values at one's disposal that are as well-founded as possible. Corresponding results are presented in this Brief Report. In the following we use the abbreviation “ZT” when we refer to the amplitudes of Zhou and Timmermans [8].

Note that $\bar{p}d$ scattering was also considered in Ref. [9] utilizing, however, the results from the old Nijmegen $\bar{p}p$ partial-wave analysis [10] from 1994.

II. RESULTS AND DISCUSSION

We study $\bar{p}d$ scattering within the Glauber theory based on the single- and double $\bar{p}N$ scattering mechanisms. The full spin dependence of the elementary $\bar{p}N$ scattering amplitudes is taken into account and both the S - and D -wave components of the deuteron are considered. Details of the formalism can be found in Refs. [3, 11], where we also provide definitions of the considered $\bar{p}d$ observables in terms of the twelve invariant amplitudes that arise for spin $1/2+1$ scattering.

The $\bar{N}N$ amplitudes of the new analysis of Zhou and Timmermans are reconstructed from the phase shifts and inelasticity parameters as given in their tables VIII-X [8]. Those values are obtained under the assumption of

isospin symmetry and, therefore, match our study where likewise isospin symmetry is imposed for the hadronic amplitude. Since only partial waves up to a total angular momentum of $J = 4$ are listed we considered two options for supplementing the contributions from higher partial waves, namely (a) one-pion exchange and (b) higher partial waves predicted by the Jülich model A. It turned out that there is very little difference in the resulting $\bar{N}N$ amplitudes, at least up to $p_{lab} = 800$ MeV/c, which is the highest momentum considered in our study. Actually, even in a test calculation of differential cross sections and analyzing powers based on the phase shifts at 900 MeV/c with our reconstructed amplitudes we obtained nice agreement with the results for $\bar{p}p$ elastic and $\bar{p}p \rightarrow \bar{n}n$ charge-exchange scattering (at $860 \approx 886$ MeV/c) displayed in Ref. [8].

Following our previous work we use a Gaussian ansatz for representing the amplitudes generated from the $\bar{N}N$ phase-shift parameters of Ref. [8] in analytical form. Again, we aim at an excellent reproduction of the original amplitudes over the whole angular range. In the $\bar{p}d$ calculation we introduce a cutoff that suppresses the amplitudes in the backward hemisphere as described in [3] and we vary the cutoff angle in the $\bar{p}d$ calculations. The bands in the figures represent the variation of the $\bar{p}d$ observables due to the procedure described above. As argued in [3], we regard these bands as a sensible guide-

line for estimating the angular region where the Glauber theory is able to provide solid results for a specific observable and where this approach starts to fail. We want to remind the reader that contributions from large angles are in contradiction with the basic approximations underlying the Glauber model and, thus, any sizable influence from them undoubtedly marks the breakdown of this approach.

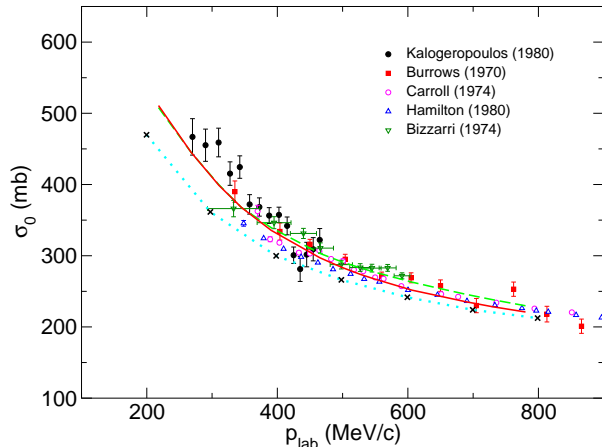


FIG. 3: (Color online) Total unpolarized $\bar{p}d$ cross section versus the antiproton laboratory momentum. Results are shown for the $\bar{N}N$ amplitudes of Ref. [8] (dotted line) and for the $\bar{N}N$ models A (dashed line) and D (solid line). Data are taken from Refs. [13–15].

First let us consider the differential cross section at 179 MeV where data are available [12], see Fig. 1. Our Glauber calculation describes the first diffractive peak quite well - for amplitudes taken from the $\bar{p}p$ partial-wave analysis as well as for those generated from the $\bar{N}N$ model D of the Jülich Group. (The result for the former is based on the amplitudes at 175.3 MeV ($p_{\text{lab}} = 600$ MeV/c) listed in Ref. [8].) Model D also explains the first minimum in the differential cross section, located at $q^2 \approx 0.12 - 0.13$ (GeV/c) 2 (i.e. $\theta_{c.m.} \approx 55^\circ$), and the onset of the second maximum whereas here the ZT $\bar{N}N$ amplitudes lead to an overestimation. The obvious strong disagreement with the data at larger transferred momenta, $q^2 > 0.15$ (GeV/c) 2 , corresponding to $\theta_{c.m.} > 60^\circ$, lies already in the region where the increase in the band widths indicates that our Glauber results are not reliable anymore, cf. the corresponding discussions in Ref. [3].

In case of the vector analyzing powers $A_y^{\bar{p}}$ and A_y^d our investigation [3] had indicated a strong model dependence. Thus, it is not surprising that the corresponding predictions for the ZT amplitudes differ from those of the Jülich models as can be seen in Fig. 2. Indeed, the ZT amplitudes yield significantly larger values for those observables. The tensor analyzing powers A_{xx} and A_{yy} were found to be much less sensitive to differences in the $\bar{N}N$ amplitudes because these observables are dominated by the spin-independent amplitudes. For the ZT

amplitudes we obtain results that exhibit an angular dependence that is very similar to the one predicted by the Jülich models. Indeed the results almost coincide with those for model A and, therefore, we do not display the latter for reasons of clarity.

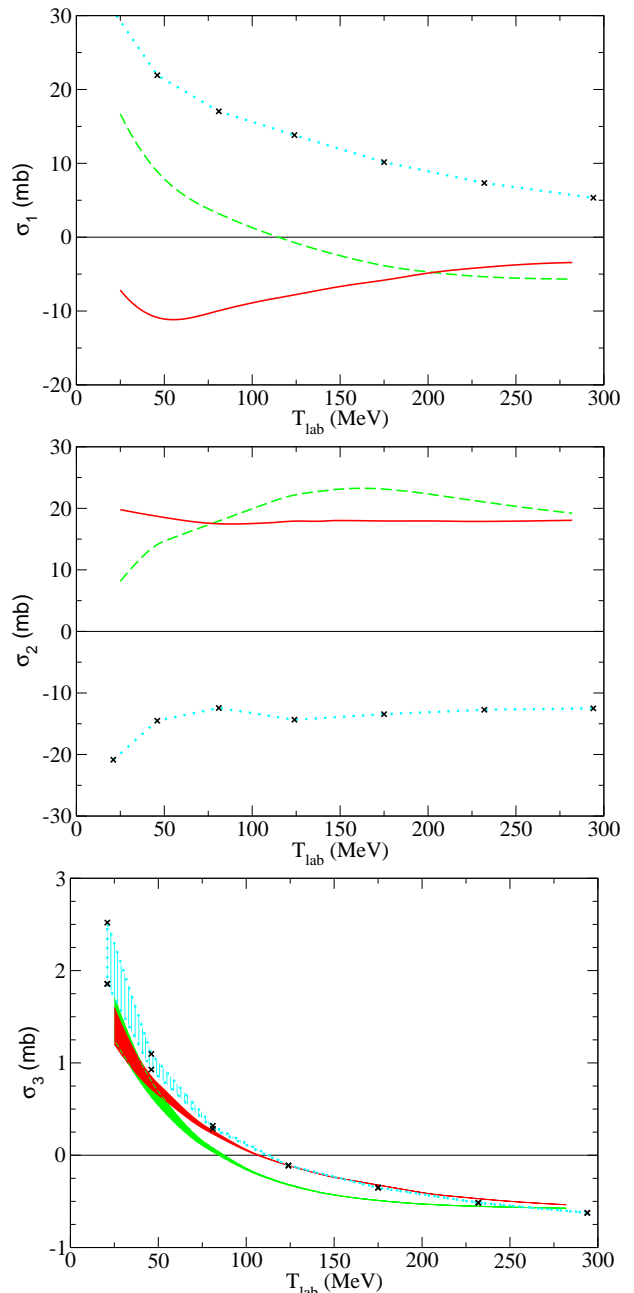


FIG. 4: (Color online) Total $\bar{p}d$ cross section σ_1 , σ_2 , and σ_3 versus the antiproton kinetic energy in the laboratory system. Same description of curves as in Fig. 3.

The total $\bar{p}d$ cross section is defined by [11]

$$\sigma = \sigma_0 + \sigma_1 \mathbf{P}^{\bar{p}} \cdot \mathbf{P}^d + \sigma_2 (\mathbf{P}^{\bar{p}} \cdot \hat{\mathbf{k}})(\mathbf{P}^d \cdot \hat{\mathbf{k}}) + \sigma_3 P_{zz}, \quad (1)$$

where $\hat{\mathbf{k}}$ is the unit vector in the direction of the antiproton beam, $\mathbf{P}^{\bar{p}}$ (\mathbf{P}^d) is the polarization vector of the

antiproton (deuteron), and P_{zz} is the tensor polarization of the deuteron ($OZ||\hat{\mathbf{k}}$). Corresponding results are presented in Figs. 3 and 4. It is obvious that the unpolarized cross section σ_0 (Fig. 3) based on the ZT amplitudes is somewhat smaller than those for the Jülich $\bar{N}N$ models. It is also below the bulk of the experimental data [13–15]. A closer inspection revealed that this difference is mainly due to a qualitative difference in the magnitude of the isospin $I = 1$ amplitude. In the Jülich models $\sigma_{\bar{p}n} \propto |T_{I=1}|^2$ is about 10–15 % larger than the result we obtain for the $I = 1$ amplitude of Ref. [8]. The $\bar{p}p$ and $\bar{p}p \rightarrow \bar{n}n$ cross sections are given by $\sigma_{\bar{p}p} \propto |(T_{I=0} + T_{I=1})/2|^2$ and $\sigma_{\bar{p}p \rightarrow \bar{n}n} \propto |(T_{I=0} - T_{I=1})/2|^2$, respectively, so that interferences between the $I = 0$ and $I = 1$ amplitudes play a role and the (absolute) size of the isospin amplitudes is not so tightly constrained. However, the $\bar{p}d$ scattering cross section is given (in the simple impulse approximation [11]) by $\sigma_{\bar{p}d} \propto (|(T_{I=0} + T_{I=1})/2|^2 + |T_{I=1}|^2)$. Note that the calculation for the ZT amplitudes was done at those energies (marked by “x” in the figures) for which the values are listed in [10]. To guide the eye we connected those points with a dotted line.

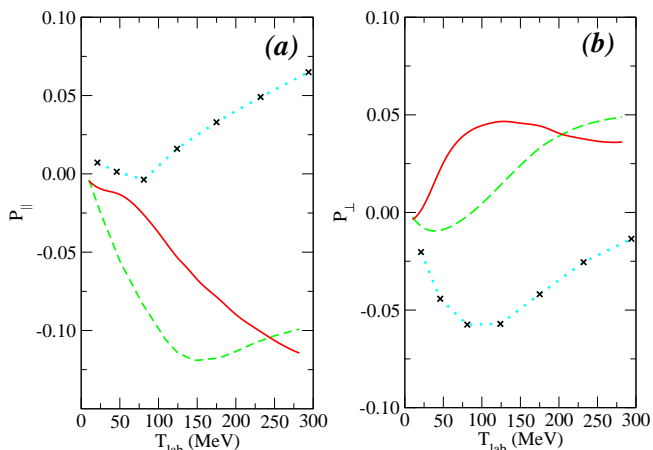


FIG. 5: (Color online) Dependence of the (a) longitudinal (P_{\parallel}) and (b) transversal (P_{\perp}) polarization on the beam energy. Same description of curves as in Fig. 3. The acceptance angle is 20 mrad.

Predictions for the spin-dependent $\bar{p}d$ cross section σ_1 , σ_2 , and σ_3 are shown in Fig. 4. Again, as for the analyzing powers discussed above, we see sizable differences in the results based on the ZT amplitudes to the ones obtained from the $\bar{N}N$ amplitudes of the Jülich models. Specifically, those cross sections are larger (σ_1) or even of opposite sign (σ_2). Only the tensor-polarized cross section σ_3 turns out to be similar for all three considered $\bar{N}N$ amplitudes.

The quantity relevant for the efficiency of the polarization buildup is the polarization degree $P_{\bar{p}}$ at the beam life time t_0 [16]. With our definition of σ_1 and σ_2 [3] this quantity is given by

$$P_{\bar{p}}(t_0) = -2P_T \frac{\sigma_1}{\sigma_0}, \text{ if } \boldsymbol{\zeta} \cdot \hat{\mathbf{k}} = 0, \\ P_{\bar{p}}(t_0) = -2P_T \frac{\sigma_1 + \sigma_2}{\sigma_0}, \text{ if } |\boldsymbol{\zeta} \cdot \hat{\mathbf{k}}| = 1, \quad (2)$$

where the unit vector $\boldsymbol{\zeta}$ is directed along the target polarization vector P_T . Results for the transversal polarization P_{\perp} ($\boldsymbol{\zeta} \cdot \hat{\mathbf{k}} = 0$) and for the longitudinal polarization P_{\parallel} ($\boldsymbol{\zeta} \cdot \hat{\mathbf{k}} = 1$) are shown in Fig. 5 for $P_T = P^d = 1$. Obviously, there are sizable differences in the predicted values for the considered $\bar{N}N$ amplitudes. But the overall magnitude – which is decisive for the polarization buildup – is comparable and in the order of 5–10 % in the energy region considered. With regard to the calculation based on the $\bar{N}N$ amplitudes from the partial-wave analysis [8] we want to point out that our results for the polarization degree for a deuterium target are smaller than those for a hydrogen target, found to be around 20 % in Ref. [17] for the acceptance angle of 20 mrad considered by us. Moreover, they are much smaller than the large values of around 30 % reported in Ref. [9] in a $\bar{p}d$ calculation that utilizes the old Nijmegen $\bar{N}N$ partial-wave analysis [10].

Acknowledgements: This work was supported in part by the Heisenberg-Landau program.

-
- [1] V. Barone *et al.*, arXiv:hep-ex/0505054.
 - [2] F. Rathmann *et al.*, Phys. Rev. Lett. **94**, 014801 (2005).
 - [3] Yu.N. Uzikov and J. Haidenbauer, Phys. Rev. C **87**, 054003 (2013).
 - [4] V. Franco and R. Glauber, Phys. Rev. **142**, 1195 (1966).
 - [5] T. Hippchen, J. Haidenbauer, K. Holinde, V. Mull, Phys. Rev. C **44**, 1323 (1991).
 - [6] V. Mull, J. Haidenbauer, T. Hippchen and K. Holinde, Phys. Rev. C **44**, 1337 (1991).
 - [7] V. Mull and K. Holinde, Phys. Rev. C **51**, 2360 (1995).
 - [8] D. Zhou and R. G. E. Timmermans, Phys. Rev. C **86**, 044003 (2012).
 - [9] S. G. Salnikov, Nucl. Phys. A **874**, 98 (2012).
 - [10] R. Timmermans, T. A. Rijken and J. J. de Swart, Phys. Rev. C **50**, 48 (1994).
 - [11] Yu.N. Uzikov and J. Haidenbauer, Phys. Rev. C **79**, 024617 (2009).
 - [12] G. Bruge *et al.*, Phys. Rev. C **37**, 1345 (1988).
 - [13] V. Flaminio *et al.*, CERN-HERA 84-01 (1984).
 - [14] A.S. Carroll *et al.*, Phys. Rev. Lett. **32**, 247 (1974).
 - [15] R. P. Hamilton, T. P. Pun, R. D. Tripp, D. M. Lazarus and H. Nicholson, Phys. Rev. Lett. **44**, 1182 (1980).
 - [16] V.F. Dmitriev, A. Milstein, S. Salnikov, Phys. Lett. B **690**, 427 (2010).
 - [17] D. Zhou and R. G. E. Timmermans, Phys. Rev. C **87**, 054005 (2013).